

Analysis of Changes in Retinal Photoreceptors Using Optical Coherence Tomography in a Feline Model of Iodoacetic Acid-induced Retinal Degeneration

Gwang Myeong Noh¹, Jae Wan Lim², Myung Shin Lee³, Seung Uk Lee¹, Sang Joon Lee¹

¹Department of Ophthalmology, Kosin University College of Medicine, Busan, Korea

²Yangsan-si Dong-myeon Local Public Health Clinic, Busan, Korea

³Department of Ophthalmology, Haeundae Paik Hospital, Inje University College of Medicine, Busan, Korea

Purpose: We investigated structural changes in the retina by using optical coherence tomography (OCT) in a feline model of retinal degeneration using iodoacetic acid (IAA).

Methods: We examined 22 eyes of 11 felines over 2 years of age. The felines had fasted for 12 hours and were intravenously injected with IAA 20 mg/kg of body weight. OCT (Spectralis OCT) was performed at the point where the ends of the retinal vessels collected in the lateral direction from the optic nerve head and area centralis. Similarly, OCT was performed four times at 1-week intervals following injections, at which point the felines were sacrificed and histologic examinations were performed. Using OCT, the thickness of each layer of the retina was measured.

Results: The average body weight of the three male and eight female felines investigated in this study was 1.61 ± 0.19 kg. The mean total retinal thickness of the felines before injection was 221.32 ± 9.82 μm , with a significant decrease in the retinal thickness at 2, 3, and 4 weeks following injections of 186.41 ± 35.42 , 174.56 ± 31.94 , and 175.35 ± 33.84 μm , respectively ($p = 0.028$, 0.027 , and 0.027 , respectively). The thickness of the outer nuclear layer was 57.49 ± 8.03 μm before injection and 29.26 ± 17.87 , 25.62 ± 13.88 , and 31.60 ± 18.38 μm at 2, 3, and 4 weeks, respectively, after injection ($p = 0.028$, 0.028 , 0.046 , respectively).

Conclusions: In a feline model of retinal degeneration using IAA, the total retinal thickness and the thickness of the outer nuclear layer were shown to decrease significantly on OCT.

Key Words: Angiography, Feline, Iodoacetic acid, Optical coherence tomography, Retinal degeneration

Retinitis pigmentosa (RP) is a typical photoreceptor-destroying retinal degenerative disease [1]. The worldwide

prevalence of RP is about 1 in 4,000, affecting more than one million individuals worldwide [2]. RP includes a diverse group of genetic disorders characterized by the degeneration of rod and cone cells [3,4]. Symptoms include night blindness and decreased peripheral vision, eventually causing the loss of central vision [1,2]. Until now, no definitive treatments have been available. New treatment methods have been explored using various animal models based

Received: July 13, 2019 Final revision: August 27, 2019

Accepted: September 6, 2019

Corresponding Author: Sang Joon Lee, MD, PhD. Department of Ophthalmology, Kosin University College of Medicine, 262 Gamcheon-ro, Seo-gu, Busan 49267, Korea. Tel: 82-51-990-6140, Fax: 82-51-990-3026, E-mail: hiatus@kosin.ac.kr

© 2019 The Korean Ophthalmological Society

This is an Open Access article distributed under the terms of the Creative Commons Attribution Non-Commercial License (<http://creativecommons.org/licenses/by-nc/3.0/>) which permits unrestricted non-commercial use, distribution, and reproduction in any medium, provided the original work is properly cited.

on the natural history of the disease [2].

Various animal models have been used to study retinal degeneration such as RP [5-8]. Among animal models, the eyes of felines and swine have a central region (comprised partly of photoreceptors) comparable to the human macula, with similar distributions of rod and cone cells in the central and peripheral retina [9]. Therefore, using iodoacetic acid (IAA), such animals have been designated as models of retinal degeneration [10-15]. IAA reacts with the sulfhydryl groups of glyceraldehyde 3-phosphate dehydrogenase (GADPH) in cells of various organs, including the eye, and inhibits anaerobic glycolysis [16-21]. Based on this mechanism, an optimal IAA concentration can selectively damage photoreceptors in the retina, which are most susceptible to hypoxia in our body. In this process, the inner retina is preserved and shows histological features that appear early in human RP [22]. Based on these characteristic findings of retinal degeneration, an animal model of IAA-induced retinal degeneration has been designed to explore effective treatment of RP disease in human eyes [10,12,14].

The genetics of retinal degeneration have been investigated in large animal models. The results of retinal degeneration using a Bengal feline model are yet to be reported. RP is inherited as an autosomal recessive disease. Degeneration occurs within one year of birth, with progressive genetic retinal atrophy [23]. Unfortunately, animal models are not easy to breed or to cultivate for the long term. Nevertheless, the development of a feline model of retinal degeneration using IAA has been reported [10]. Retinal degeneration has been successfully induced with adequate IAA [10]. In that research, however, the time of induction of retinal degeneration before and after IAA injection or changes in photoreceptor cells were not confirmed histologically.

Optical coherence tomography (OCT), which is widely used in ophthalmology, is a noninvasive, non-contact technique for acquisition of images of the retina and the optic nerve through the pupil. It provides a high-resolution cross-sectional image [15]. Despite attempts to analyze retinal degeneration in animal models with OCT, studies involving models of feline retinal degeneration have yet to be reported [12,24]. In the present study, we evaluate whether structural changes in the retina observed with OCT correlate chronologically with histological examination following IAA induction.

Materials and Methods

Animal subjects

This study is based on a total of 22 eyes from 11 adult felines (three males and eight females) of at least 2 years of age. Experimental groups included a normal control group of four eyes (one male and one female) and a group of 18 eyes (two males and seven females) showing retinal degeneration. Felines were acquired after quarantine at Gyeongsang National University College of Veterinary Medicine, and in accordance with the guidelines for animal experiments as prescribed by the Association for Research in Vision and Ophthalmology (ARVO). The animals were housed in an animal laboratory operated by our medical school. The above experiment was carried out after formal approval from the Animal Experimental Ethics Committee (Kosin 13-15). We minimized pain and discomfort in the animal subjects according to the guidelines of the ARVO Statement for the Use of Animals in Ophthalmic and Vision Research.

Induction of retinal degeneration by iodine acetic acid injection

IAA (Sigma-Aldrich, Buchs, Switzerland) was dissolved in 10 milliliters (mL) of phosphate-buffered saline (Lonza, Walkersville, MD, USA), and the pH was adjusted to 7.4. The solution was then passed through a 0.2- μ m filter (Minisart, Sartorius Stedim, Biotech, Germany). A 20-mg/kg dose of IAA was slowly injected into the femoral veins of subjects using a 24-gauge needle over the course of 5 minutes.

Measurement of body weight, axial length, and fasting blood glucose

The felines were injected with 3.5 mg/kg of tiletamine hydrochloride, 10 mg/kg of Zoletil 50 (Virbac SA, Carros Cedex, France), and 3.5 mg/kg of hydrochloric acid xylazine (Rompun, Bayer, Leverkusen, Germany) for anesthesia. After anesthesia was administered, body weight and axial length were measured.

Weights were measured with an electronic balance (Entris5201, Sartorius, Göttingen, Germany). The axial length, from the anterior surface of the cornea to the retinal pig-

ment epithelium, was measured using A-scan ultrasound biometry (A-scan) (Quantel Medical, France). The axial length was measured 10 times, and the mean value was obtained without pressing the central cornea under anesthesia. Blood glucose was measured after fasting for 12 hours (Accu-Chek, Roche Diagnostics, Mannheim, Germany).

Fluorescein angiography

Using Heidelberg Spectralis retinal angiography (Heidelberg Engineering, Heidelberg, Germany), fundus angiographies were twice performed, once before IAA injection and again 4 weeks later. A fluorescent agent (10 mg/kg body weight; Fluorescite, Alcon, Tokyo, Japan) was injected through the femoral veins of anesthetized felines, followed eventually by retinal angiography. Angiography was started shortly after injection and lasted about 7 to 8 minutes.

Retinal thickness using OCT

The retina was photographed using an OCT machine. The felines were treated with 0.5% tropicamide and 0.5% phenylephrine eye drops (Mydrin-P, Santen, Japan) four times at 10-minute intervals for mydriasis. OCT was performed using the Spectralis OCT (Heidelberg Engineering) before IAA injection and again after 1, 2, 3, and 4 weeks. The observed central region spanned from the optic disc head laterally to the retinal vascular arcade (Fig. 1A-1C). The imaging speed of OCT was 40,000 A-scan per second. The volume scan consisted of a linear scan (8.9 mm in width and 1.9 mm in depth). A total of 25 such linear scans, each 6 mm in width and 1.9 mm in depth, were performed. Using an automated real-time function for eye tracking, the retina was always photographed in the same position. All the scans with a signal strength of 80 frames or more were included in the results to obtain a good image. Recorded OCT images were stored in a JPG file of maximum image quality using Heidelberg Eye Explorer vers. 1.8.6 (Heidelberg Engineering).

Using these image files, the gray value graph was obtained using the Plot Profile function of the ImageJ program ver. 1.47 (National Institutes of Health, Bethesda, MD, USA). Photoreceptor thicknesses were determined according to the gray scale values of the retinal pigment

epithelium, the photoreceptor inner and outer segments, and the external limiting membrane. The boundaries between the outer nuclear layer, the outer plexiform layer, the inner nuclear layer, the inner plexiform layer, the ganglion cell layer, and the nerve fiber layer showed the maximum change in graph slope (Fig. 1C). The thickness of each layer was determined as the average of three measurements. Fig. 1C is a reconstruction of a gray value graph obtained from the ImageJ program with GraphPad Prism ver. 7.02 (GraphPad Software, La Jolla, CA, USA). Central retinal thickness was measured using the macular thickness map function embedded in Heidelberg Eye Ex-

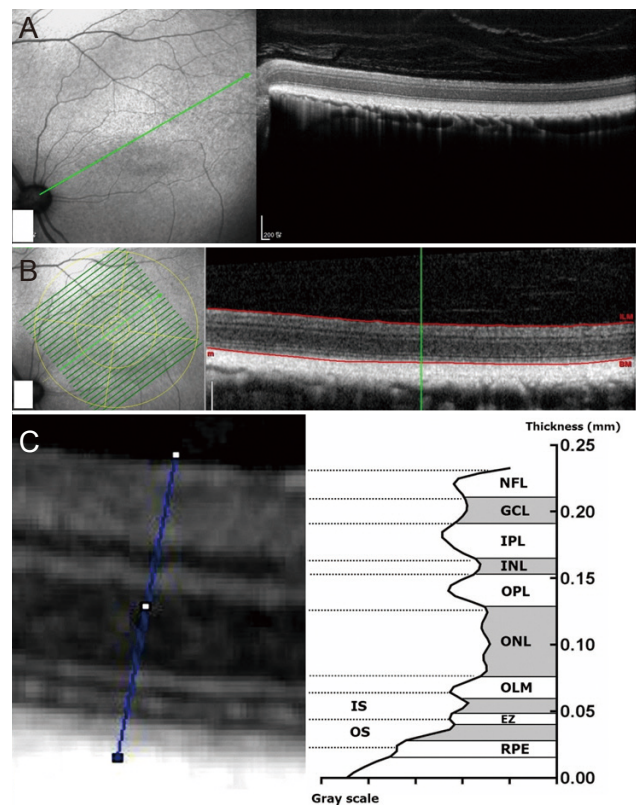


Fig. 1. Optical coherence tomography imaging. Spectralis optical coherence tomography was used to image the area centralis, where the vessel ends meet. (A) Linear scan. (B) Volume scan. Early Treatment for Diabetic Retinopathy Study circle shown in yellow line. (C) Measuring each retinal layer thickness. The thickness of each retinal layer was measured using ImageJ gray-scale. The above graph was obtained using GraphPad Prism program ver. 7.02. NFL = nerve fiber layer; GCL = ganglion cell layer; IPL = inner plexiform layer; INL = inner nuclear layer; OPL = outer plexiform layer; ONL = outer nuclear layer; OLM = outer limiting membrane; IS = inner segment layer; OS = outer segment layer; EZ = ellipsoid zone; RPE = retinal pigmented epithelium.

plorer ver. 1.8.6 (Heidelberg Engineering). Retinal thickness was measured in a single retinal section using the ImageJ program described above.

Histologic evaluation using hematoxylin and eosin stain

Each feline was sacrificed using carbon dioxide, and the eyeballs were removed. Each cornea, iris, lens, and vitreous body were separated without incurring retinal damage following a circular incision along the corneal limbus. The optic nerve was placed on the floor and a horizontal incision was made along the tapetum lucidum border and the inferior margin of the optic nerve. A vertical incision of 90° including the medial margin of the optic nerve was performed based on this line. Tissue samples measuring 6 mm × 6 mm with the full thickness of neurosensory retina to sclera, including the optic nerve, were obtained. The tissue was fixed in 10% formalin (Formaldehyde, GoldenBio-tech Co., Seoul, Korea) solution for 48 hours. Fixed tissues were paraffin-embedded, serially sectioned with a paraffin-embedded microtome (Leica RM2235, Nussloch, Baden-Württemberg, Germany) to obtain 4-µm-thick slices, and tissue slides were prepared.

Paraffin-embedded tissue specimens on slides were twice treated with xylene for 5 minutes (a process of deparaffinization). The sections were twice treated with 100% ethanol for 5 minutes and were treated once, for 5 minutes each, with 95%, 80%, and 70% ethanol. The sections were washed for 5 minutes with phosphate-buffered saline. Sections were dyed with hematoxylin (Poly Scientific, Cleveland Avenue, NY, USA) for 5 minutes, and with eosin (Poly Scientific) for 3 minutes. The slides were treated with 70%, 80%, and 95% ethanol once for 2 minutes each, twice with 100% ethanol for 2 minutes each, and twice with xylene for 5 minutes each. The tissues were examined with an optical microscope (Eclipse 80i, Nikon, Kawasaki, Japan). The thickness of the outer nuclear layer was measured at 2,000 µm temporal from the optic disc.

Statistical analysis

Thicknesses of each retinal layer at injection and at 1, 2, 3, and 4 weeks after injection were compared using Wilcoxon signed-rank tests. The thickness of the outer granular layer of histologic examination, the area of the rod cells

under the immunochemical stain, and the number of cells per unit length of cone cells were measured using PASW Statistics ver. 18.0 (SPSS Inc., Chicago, IL, USA). Based on Wilcoxon signed-rank tests, a value of $p < 0.05$ was considered statistically significant.

Results

Weight, axial length, and fasting blood glucose results

The average weight of the felines was 1.61 ± 0.19 kg, the mean axial length was 19.25 ± 0.67 mm, and the mean fasting blood glucose before IAA injection was 146.61 ± 25.02 mg/dL (Table 1).

Table 1. Baseline characteristics of felines

Baseline characteristics	Control (n = 2)	IAA group (n = 9)
Weight (kg)	1.75 ± 0.35	1.61 ± 0.19
Sex (male : female)	1 : 1	2 : 7
Axial length (mm)	19.13 ± 0.31	19.25 ± 0.67
Fasting glucose (mg/dL)	144.5 ± 4.95	146.61 ± 25.02

Values are presented as mean ± standard deviation or number. IAA = iodoacetic acid.

Fluorescein angiography

Fluorescein angiography performed before IAA injection and at 4 weeks after injection revealed only a delayed leak around the blood vessels after injection in feline number 4. Following injection of fluorescein in the fundus prior to IAA injection, the arterial, arteriovenous, and venous phases were gradually attenuated. The latency time was approximately 9 ± 0.82 seconds. The retinal arterial phase started at 10 ± 0.81 seconds after fluorescein dye administration. The retinal arteriovenous phase started at 14 ± 0.96 seconds, and the retinal venous phase started at 17.25 ± 1.26 seconds after administration. The same pattern was observed after injection (Fig. 2A-2D). No differences were observed before and after injection in any of the other felines. However, multiple hyperfluorescent dots were observed in the late phase in feline number 4 injected with IAA (Fig. 2B).

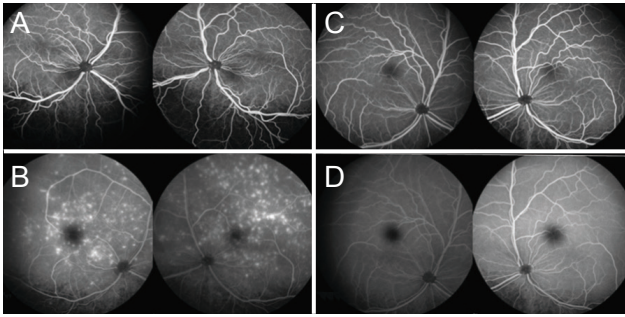


Fig. 2. (A,B) Fluorescein angiography results from feline 4. (A) No abnormalities of the retina before iodoacetic acid (IAA) injection at 2:49, 2:26 seconds. (B) Delayed leak around the central and peripheral retina after IAA injection at 6:12, 7:08 seconds. (C,D) Fluorescein angiography results from feline 5. (C) No retinal abnormalities before IAA injection (at 3:12, 1:00 seconds after fluorescein injection). (D) No interval changes after IAA injection (at 1:09, 5:22 seconds after fluorescein injection).

Retinal degeneration findings based on OCT

Structures corresponding to the retinal nerve fiber layer, ganglion cell layer, inner plexiform layer, inner nuclear layer, outer plexiform layer, outer nuclear layer, external limiting membrane, and junction of the inner and outer photoreceptor segments were observed prior to IAA injection (Fig. 3A). Mean thicknesses of the outer nuclear layer before and at 1, 2, 3, and 4 weeks after IAA injection were 57.49 ± 8.03 , 36.12 ± 18.91 , 29.26 ± 17.87 , 25.62 ± 13.88 , and 31.60 ± 18.38 μm , respectively. The thickness of the outer nuclear layer decreased significantly at 1, 2, 3, and 4 weeks after IAA injection compared to pre-injection levels in this group ($p = 0.075$, $p = 0.028$, $p = 0.028$, and $p = 0.046$, respectively) (Fig. 3B-3E).

Analysis of changes in retinal thickness by OCT

The mean retinal thickness of the felines measured by OCT was 221.32 ± 9.82 μm , and retinal thicknesses at 1, 2, 3, and 4 weeks after injection were 207.34 ± 23.36 , 186.41 ± 35.42 , 174.56 ± 31.94 , and 175.35 ± 33.84 μm , respectively. The retinal thickness was significantly decreased at 2, 3, and 4 weeks ($p = 0.028$, 0.027 , and 0.027 , respectively). The central retinal thickness was 227.65 ± 13.36 μm before injection and 211.33 ± 18.26 , 181.03 ± 21.33 , 165.32 ± 14.21 , and 168.72 ± 18.74 μm when measured at 1, 2, 3, and 4 weeks, respectively, following injection ($p = 0.031$, 0.016 , and 0.024 , respectively). The thickness of the outer nuclear layer was 57.49 ± 8.03 μm before injection, and $29.26 \pm$

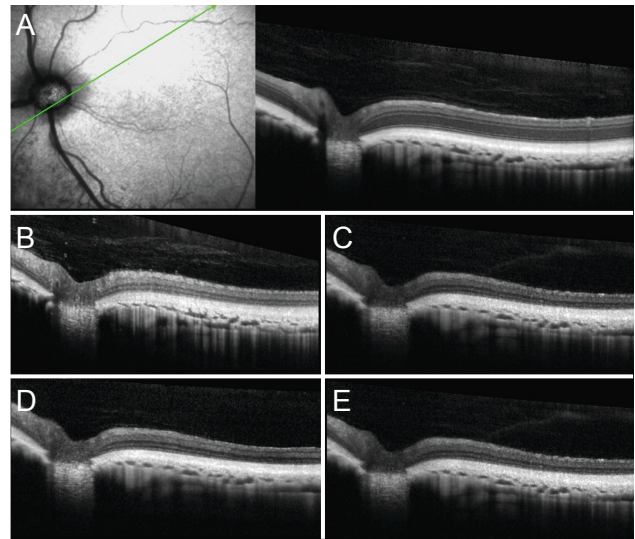


Fig. 3. Retinal changes obtained with optical coherence tomography after iodoacetic acid injection. (A) Baseline. (B) First week after injection. (C) Second week after injection. (D) Third week after injection. (E) Fourth week after injection. Note that the outer nuclear layer was substantially reduced and the photoreceptor layer was degenerated.

17.87 , 25.62 ± 13.88 , and 31.60 ± 18.38 μm at 2, 3, and 4 weeks after injection, respectively ($p = 0.028$, 0.028 , and 0.046 , respectively) (Table 2 and Fig. 4).

Histologic evaluation

Optical microscopy revealed that the thickness of the outer nuclear layer was markedly reduced, and inner segment/outer segment junctions were obscured by degeneration of the photoreceptors (Fig. 5A, 5B). The thickness of each retinal layer in IAA-treated feline retinas varied as follows. The mean total retinal thickness was 175.23 ± 33.73 μm . Thicknesses of the outer segment layer, the inner segment layer, the outer nuclear layer, the outer plexiform layer, the inner nuclear layer, the inner plexiform layer, the ganglion cell layer, and the nerve fiber layer were 24.07 ± 11.06 , 20.06 ± 5.67 , 31.43 ± 18.19 , 21.40 ± 4.14 , 18.72 ± 4.85 , 30.76 ± 4.85 , 17.38 ± 4.14 , and 22.07 ± 6.59 μm , respectively. The total retinal thickness in the normal group was 207.07 ± 1.29 μm . The thicknesses of different retinal layers in the normal control group were as follows: outer segment layer, 30.38 ± 0.81 μm ; inner segment layer, 21.31 ± 0.64 μm ; outer nuclear layer, 51.32 ± 7.26 μm ; outer plexiform layer, 21.73 ± 0.73 μm ; inner nuclear layer, 19.55 ± 0.15 μm ; inner plexiform layer, 34.14 ± 1.86 μm ; ganglion cell layer, $19.74 \pm$

Table 2. Changes in thickness of each retinal layer after iodoacetic acid injection measured with optical coherence tomography imaging (n = 18)

Retinal layer (μm)	Baseline	1st week*	2nd week*	3rd week*	4th week*
Central retina thickness [†]	227.65 \pm 13.36	211.11 \pm 18.26 (<i>p</i> = 0.215)	181.03 \pm 21.33 (<i>p</i> = 0.031)	165.32 \pm 14.21 (<i>p</i> = 0.016)	168.72 \pm 18.74 (<i>p</i> = 0.024)
Total retinal thickness [‡]	221.32 \pm 9.82	207.34 \pm 23.36 (<i>p</i> = 0.223)	186.41 \pm 35.42 (<i>p</i> = 0.028)	174.46 \pm 31.94 (<i>p</i> = 0.027)	175.35 \pm 33.84 (<i>p</i> = 0.027)
OS [‡]	31.48 \pm 4.17	28.90 \pm 9.12 (<i>p</i> = 0.126)	24.73 \pm 10.55 (<i>p</i> = 0.079)	27.68 \pm 6.49 (<i>p</i> = 0.134)	24.17 \pm 11.14 (<i>p</i> = 0.069)
IS [‡]	20.86 \pm 3.98	16.76 \pm 4.07 (<i>p</i> = 0.116)	21.23 \pm 9.06 (<i>p</i> = 0.192)	18.21 \pm 4.34 (<i>p</i> = 0.211)	20.44 \pm 5.96 (<i>p</i> = 0.723)
ONL [‡]	57.49 \pm 8.03	36.12 \pm 18.91 (<i>p</i> = 0.075)	29.26 \pm 17.87 (<i>p</i> = 0.028)	25.62 \pm 13.88 (<i>p</i> = 0.028)	31.60 \pm 18.38 (<i>p</i> = 0.046)
OPL [‡]	22.22 \pm 4.11	20.75 \pm 2.87 (<i>p</i> = 0.465)	24.25 \pm 6.19 (<i>p</i> = 0.501)	20.21 \pm 8.99 (<i>p</i> = 0.686)	21.54 \pm 4.24 (<i>p</i> = 0.674)
INL [‡]	19.51 \pm 5.90	26.26 \pm 8.34 (<i>p</i> = 0.116)	18.77 \pm 5.00 (<i>p</i> = 0.511)	21.56 \pm 6.35 (<i>p</i> = 0.587)	18.85 \pm 5.09 (<i>p</i> = 0.686)
IPL [‡]	35.45 \pm 5.07	36.82 \pm 5.90 (<i>p</i> = 0.475)	37.23 \pm 5.82 (<i>p</i> = 0.317)	35.58 \pm 5.29 (<i>p</i> = 0.362)	30.93 \pm 4.94 (<i>p</i> = 0.527)
GCL [‡]	22.97 \pm 7.08	18.88 \pm 3.45 (<i>p</i> = 0.138)	17.62 \pm 4.18 (<i>p</i> = 0.087)	18.10 \pm 6.25 (<i>p</i> = 0.345)	17.57 \pm 4.23 (<i>p</i> = 0.108)
NFL [‡]	20.19 \pm 4.97	22.11 \pm 6.50 (<i>p</i> = 0.463)	20.78 \pm 2.94 (<i>p</i> = 0.715)	19.49 \pm 3.08 (<i>p</i> = 0.715)	22.25 \pm 6.50 (<i>p</i> = 0.345)

Values are presented as mean \pm standard deviation.

OS = outer segment layer; IS = inner segment layer; ONL = outer nuclear layer; OPL = outer plexiform layer; INL = inner nuclear layer; IPL = inner plexiform layer; GCL = ganglion cell layer; NFL = nerve fiber layer.

*Comparison between baseline and each week. The *p*-value was based on Wilcoxon signed-rank tests; [†]Central retinal thickness was measured with Heidelberg Eye Explorer ver. 1.8.6; [‡]Total retinal thickness and thickness of each retinal layer were measured via the ImageJ program ver. 1.47.

2.98 μm ; and nerve fiber layer, 21.15 \pm 1.37 μm . Compared to the macular area in a normal feline, the total retinal thickness and the thickness of the outer nuclear layers were significantly lower.

Discussion

This study developed a retinal degeneration model using IAA in felines with binocular vision. Degeneration findings were confirmed with OCT and histology. IAA-induced felines represent large animal models of retinal degeneration. Large animals exhibit a retinal structure similar to that of humans. The distribution of rods and cones in the central and peripheral retina, where photoreceptors are concentrated, is also similar to that of humans [9,24,25]. Therefore, several investigators are currently

working toward developing larger animal models.

Genetic and chemically-induced models of retinal degeneration are available [23,26,27]. Ofri et al. [23] developed a model of progressive retinal atrophy inherited as an autosomal recessive disease that manifests degeneration within one year of birth. Graymore and Tansley [26] developed a rat model by intravenously injecting IAA. Rosch et al. [27] induced retinal degeneration in mice via IAA injection. Additionally, that research characterizes the effects of intravitreal IAA injections compared to systemic application (intraperitoneal vs. intravenous) to induce retinal degeneration. Scott et al. [11] reported that intravenous injection of IAA into swine models at 5, 7.5, 10, and 12 mg/kg reduced the length of photoreceptors and decreased the thickness of the outer nuclear layer in a dose-dependent manner. Large genetic models are associated with several disadvantages, such as difficulty of breeding, high experi-

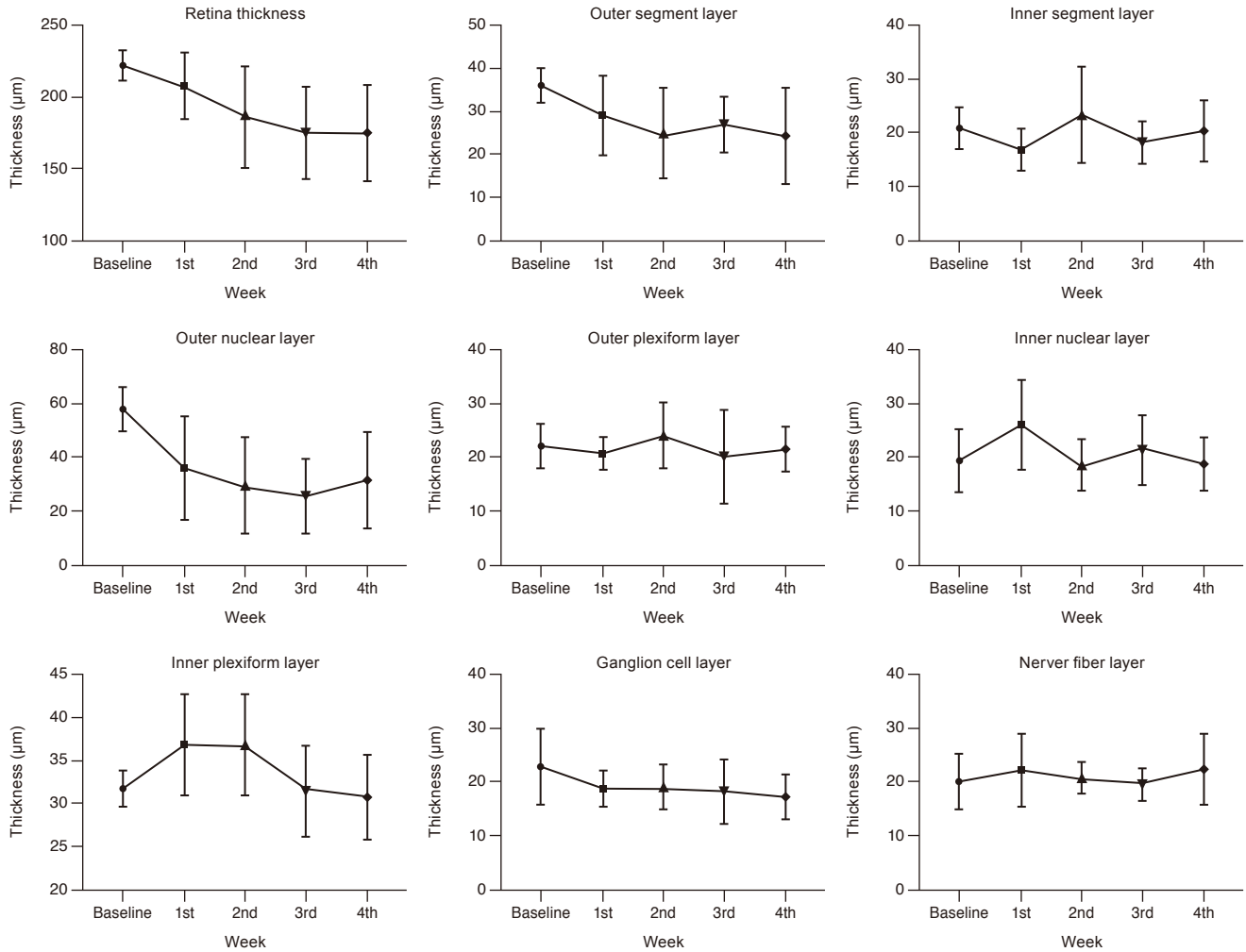


Fig. 4. Changes in retinal layer thickness after iodoacetic acid injection. * $p < 0.05$ versus baseline. Using methods shown in Fig. 1 and 2, retinal thicknesses were measured with optical coherence tomography and represented as a line graph.

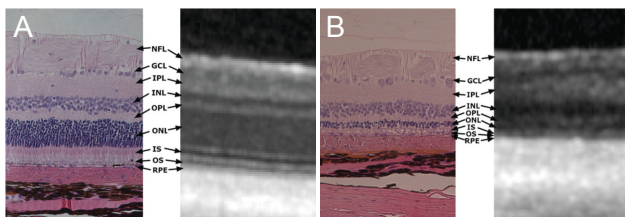


Fig. 5. Sections of normal and iodoacetic acid-treated feline retinas. A standard hematoxylin-eosin-stained retinal section matched the optical coherence tomography image. (A) Normal control. (B) An iodoacetic acid-treated feline retinal section. Outer nuclear layer thickness was reduced and outer segment/inner segment virtually disappeared. NFL = nerve fiber layer; GCL = ganglion cell layer; IPL = inner plexiform layer; INL = inner nuclear layer; OPL = outer plexiform layer; ONL = outer nuclear layer; IS = inner segment layer; OS = outer segment layer; RPE = retinal pigmented epithelium.

mental cost, and varying patterns of inheritance. The short lifespan of mouse and rat models limits our ability to predict the degree of retinal degeneration during survival periods following drug administration [26-28]. Chemical models developed via chemical injection into the vitreous have been shown to locally affect all the layers of neurosensory retina, and are therefore not useful in studies investigating outer retinal degeneration [26-28]. Further, drug doses may vary between experimental animals, along with the degree of retinal degeneration in each eye [29]. To overcome the limitations of previous retinal degeneration models, large animal models of retinal degeneration that are readily available and monitored using *in vivo* biometry techniques, such as OCT, are needed.

In the past, retinal degeneration was mainly confirmed

by histological examination. Studies investigating retinal degeneration have used electron microscopy, immunohistochemistry, electroretinography, and OCT [10,22,26]. OCT is performed using infrared interference with a wavelength of about 830 nm, which is generated using a super luminescent diode. This image is directly related to histological findings and is referred to as *in vivo* microscopy [30,31]. The junction between inner and outer segments of photoreceptors corresponds to the ellipsoid zone, while the outer end of the cone cell corresponds to the interdigitation zone surrounded by apical protrusions of the retinal pigment epithelium in human OCT findings [32]. In terms of the retina of felines, the cone sheath of a feline differs from that of a human [33]. Therefore, a third high reflection line is typically not observed. In a study of dogs and pigs using OCT, three high-reflectance lines were detected outside the outer nuclear layer [34,35]. In contrast, four highly reflective lines have been observed in some birds [36]. A bird has a central fovea and cone cells similar to a human, but the retinal structure varies depending on the bird species. It is difficult to conclude that this finding is consistent with each retinal layer observed in human OCT findings. The current study demonstrates the correlation between histologic evaluation sections and OCT in feline retinal layers. In the feline macula, the third hyper-reflective line was absent, but other layers such as the ellipsoidal zone, the retinal pigment epithelium, the outer plexiform layer, the inner plexiform layer, and the nerve fiber layer were observed and used to measure retinal degeneration.

Compared with previous studies, the greatest advantage of our study is that the retinal degeneration model was developed with IAA using a large animal with binocular vision, and that these changes were periodically observed through OCT. In the feline model of retinal degeneration using IAA herein, OCT showed a significant decrease in total retinal thickness and outer nuclear layer thickness. The total retinal thickness and the thickness of the outer nuclear layer decreased during the first 3 weeks after IAA injection, and then increased slightly at 4 weeks after IAA injection.

Fluorescein angiography was performed before injection and 4 weeks after injection. Local leakage at depigmented spots has been reported in a rodent model of retinal degeneration using fluorescein angiography [24]. A different study in Japan compared findings from indocyanine green angiography and fluorescein angiography in normal cats

[37]. Compared to human values, these outcomes were shown to be relatively slow to appear [37]. In our study, fluorescein angiography was performed prior to IAA injection and 4 weeks following injection, without any difference between pre-injection and post-injection outcomes in all but one of the felines. Only a single feline (number 4) out of nine felines displayed multiple hyperfluorescent dots around the blood vessels during the post-injection late phase. The starting time of each phase after administration of fluorescein dye was determined. Compared with humans, there was no significant difference in time between circulating phases. Data related to fundus angiography in felines showing retinal degeneration represent a novel finding, but further research is needed.

In a study of an IAA-induced swine model of retinal degeneration by Wang et al. [12], the number of rod cells decreased after 2 weeks post-injection, whereas the number of cone cells remained unchanged at 5 weeks. The rod cells had died, but it was presumed that the disappearance of IAA caused cone cell glycolysis, which led to cone cell recovery [10]. The recovery of retinal thickness at 4 weeks was also induced by selectively damaging the rod cells in this study. Wang et al. [12] proposed two mechanisms for these findings. First, glyceraldehyde GAPDH may have been re-synthesized when the concentrations in the body declined. Second, GAPDH may have been restored by sugar storage [11].

In patients with RP, the outer photoreceptor layer disappears initially, followed by the inner layer and nuclei [26,28]. Histological findings of IAA-induced retinal degeneration are similar to those of RP. Hartong et al. [2] reported that degeneration of rod cells precedes degeneration of cone cells in patients with RP. Menghini et al. [38] measured the density of cone cells in patients with RP and healthy subjects using adaptive optics scanning laser ophthalmoscopy. Adaptive optics scanning laser ophthalmoscopy findings have shown a significant positive correlation between the density of cone cells and the thickness of the outer nuclear layer in normal eyes and in eyes with RP [38]. The degree of reduction in the outer nuclear layer reflects retinal degeneration, which is confirmed by our study and consistent with actual histological changes.

At a dose of 20 mg/kg IAA, the total retinal thickness, and the thickness of the outer nuclear layer were significantly decreased on OCT at 2, 3, and 4 weeks, which was confirmed histologically. IAA modifies and inhibits GAP-

DH, thereby blocking glycolysis [29]. Neurons depend on glycolysis for adenosine triphosphate production, and photoreceptors are particularly sensitive to IAA because of their high metabolic rate [22]. This phenomenon explains why, as observed herein, the outer nuclear layer, which contains nuclei of photoreceptor neurons, lost cells while the inner retinal neurons were unaffected by IAA. Furthermore, exposure to IAA shortened the outer segment layers. The results suggest that IAA treatment specifically eliminates photoreceptors in the retina.

One limitation of this study is that it does not compare OCT outcomes and histologic findings at 1, 2, and 3 weeks after injection because the felines were sacrificed at 4 weeks. OCT shows the structure of the retina, but shows limited differentiation of rod and cone cells. Studies, including electrophysiological examination of felines, are needed to analyze the function of each photoreceptor cell. In this experiment, the number of controls was also a limitation. Nevertheless, unlike genetic models of retinal degeneration, the primary strength of this study is the relatively short period of time required to develop a model of retinal degeneration. The model is expected to serve as a large animal model of retinal degeneration.

In summary, using this model in other studies may facilitate the investigation of retinal degeneration by OCT without sacrificing experimental animals for histological examination. For example, in an experiment to determine the efficacy of a therapeutic agent, the model may be used to study retinal changes before and after treatment. This model has the potential to be used to generate basic data for retinal degeneration research. The findings of photoreceptor degeneration in felines, as confirmed by this study, will be useful for treatment and research in retinal degeneration going forward.

Conflict of Interest

No potential conflict of interest relevant to this article was reported.

Acknowledgements

This study was supported by the Basic Research Program through the National Research Foundation of Korea

(NRF) funded by the Ministry of Science, ICT & Future Planning (2017R1A2B4004664).

References

1. Berson EL. Retinitis pigmentosa. The Friedenwald lecture. *Invest Ophthalmol Vis Sci* 1993;34:1659-76.
2. Hartong DT, Berson EL, Dryja TP. Retinitis pigmentosa. *Lancet* 2006;368:1795-809.
3. Birch DG, Anderson JL, Fish GE. Yearly rates of rod and cone functional loss in retinitis pigmentosa and cone-rod dystrophy. *Ophthalmology* 1999;106:258-68.
4. Clarke G, Collins RA, Leavitt BR, et al. A one-hit model of cell death in inherited neuronal degenerations. *Nature* 2000;406:195-9.
5. Cheng YP, Ke CY, Kuo CC, Lee YJ. Effect of a complex lutein formula in an animal model for light-induced retinal degeneration. *Chin J Physiol* 2016;59:202-9.
6. Taylor L, Arner K, Ghosh F. N-methyl-N-nitrosourea-induced neuronal cell death in a large animal model of retinal degeneration in vitro. *Exp Eye Res* 2016;148:55-64.
7. Nagar S, Krishnamoorthy V, Cherukuri P, et al. Early remodeling in an inducible animal model of retinal degeneration. *Neuroscience* 2009;160:517-29.
8. Yamauchi Y, Agawa T, Tsukahara R, et al. Correlation between high-resolution optical coherence tomography (OCT) images and histopathology in an iodoacetic acid-induced model of retinal degeneration in rabbits. *Br J Ophthalmol* 2011;95:1157-60.
9. Rapaport DH, Stone J. The area centralis of the retina in the cat and other mammals: focal point for function and development of the visual system. *Neuroscience* 1984;11:289-301.
10. Nan Y, Zhang Q, Ren C, et al. Functional evaluation of iodoacetic acid induced photoreceptor degeneration in the cat. *Sci China Life Sci* 2013;56:524-30.
11. Scott PA, Kaplan HJ, Sandell JH. Anatomical evidence of photoreceptor degeneration induced by iodoacetic acid in the porcine eye. *Exp Eye Res* 2011;93:513-27.
12. Wang W, Fernandez de Castro J, Vukmanic E, et al. Selective rod degeneration and partial cone inactivation characterize an iodoacetic acid model of Swine retinal degeneration. *Invest Ophthalmol Vis Sci* 2011;52:7917-23.
13. Noel JM, Fernandez de Castro JP, Demarco PJ Jr, et al. Iodoacetic acid, but not sodium iodate, creates an inducible swine model of photoreceptor damage. *Exp Eye Res*

- 2012;97:137-47.
14. Wang Y, Zhao L, Lu F, et al. Retinoprotective effects of bilberry anthocyanins via antioxidant, anti-inflammatory, and anti-apoptotic mechanisms in a visible light-induced retinal degeneration model in pigmented rabbits. *Molecules* 2015;20:22395-410.
 15. Aplin FP, Luu CD, Vessey KA, et al. ATP-induced photoreceptor death in a feline model of retinal degeneration. *Invest Ophthalmol Vis Sci* 2014;55:8319-29.
 16. Cibis PA, Noell WK. Cataract induced by iodoacetic acid; a preliminary report. *Am J Ophthalmol* 1955;40:379-82.
 17. Orzalesi N, Calabria GA, Grignolo A. Experimental degeneration of the rabbit retina induced by iodoacetic acid: a study of the ultrastructure, the rhodopsin cycle and the uptake of ¹⁴C-labeled iodoacetic acid. *Exp Eye Res* 1970;9:246-53.
 18. Toda N. Calcium independent contraction induced by iodoacetic acid in isolated cerebral arteries. *Stroke* 1984;15:475-80.
 19. Suna H, Arai M, Tsubotani Y, et al. Dysideamine, a new sesquiterpene aminoquinone, protects hippocampal neuronal cells against iodoacetic acid-induced cell death. *Bioorg Med Chem* 2009;17:3968-72.
 20. Zhou X, Zhu L, Wang L, et al. Protective effect of edaravone in primary cerebellar granule neurons against iodoacetic acid-induced cell injury. *Oxid Med Cell Longev* 2015;2015:606981.
 21. Winkler BS, Sauer MW, Starnes CA. Modulation of the Pasteur effect in retinal cells: implications for understanding compensatory metabolic mechanisms. *Exp Eye Res* 2003;76:715-23.
 22. Noell WK. Experimentally induced toxic effects on structure and function of visual cells and pigment epithelium. *Am J Ophthalmol* 1953;36:103-16.
 23. Ofri R, Reilly CM, Maggs DJ, et al. Characterization of an early-onset, autosomal recessive, progressive retinal degeneration in Bengal cats. *Invest Ophthalmol Vis Sci* 2015;56:5299-308.
 24. Chang B. Mouse models for studies of retinal degeneration and diseases. *Methods Mol Biol* 2013;935:27-39.
 25. Ehrenberg M, Ehrenberg S, Schwob O, Benny O. Murine fundus fluorescein angiography: an alternative approach using a handheld camera. *Exp Eye Res* 2016;148:74-8.
 26. Graymore C, Tansley K. Iodoacetate poisoning of the rat retina. II. Glycolysis in the poisoned retina. *Br J Ophthalmol* 1959;43:486-93.
 27. Rosch S, Johnen S, Mazinani B, et al. The effects of iodoacetic acid on the mouse retina. *Graefes Arch Clin Exp Ophthalmol* 2015;253:25-35.
 28. Graymore C, Tansley K. Iodoacetate poisoning of the rat retina. I. Production of retinal degeneration. *Br J Ophthalmol* 1959;43:177-85.
 29. Liang L, Katagiri Y, Franco LM, et al. Long-term cellular and regional specificity of the photoreceptor toxin, iodoacetic acid (IAA), in the rabbit retina. *Vis Neurosci* 2008;25:167-77.
 30. Thomas D, Duguid G. Optical coherence tomography: a review of the principles and contemporary uses in retinal investigation. *Eye (Lond)* 2004;18:561-70.
 31. Huang D, Swanson EA, Lin CP, et al. Optical coherence tomography. *Science* 1991;254:1178-81.
 32. Spaide RF, Curcio CA. Anatomical correlates to the bands seen in the outer retina by optical coherence tomography: literature review and model. *Retina* 2011;31:1609-19.
 33. Fisher SK, Steinberg RH. Origin and organization of pigment epithelial apical projections to cones in cat retina. *J Comp Neurol* 1982;206:131-45.
 34. Hernandez-Merino E, Kecova H, Jacobson SJ, et al. Spectral domain optical coherence tomography (SD-OCT) assessment of the healthy female canine retina and optic nerve. *Vet Ophthalmol* 2011;14:400-5.
 35. Gloesmann M, Hermann B, Schubert C, et al. Histologic correlation of pig retina radial stratification with ultra-high-resolution optical coherence tomography. *Invest Ophthalmol Vis Sci* 2003;44:1696-703.
 36. Rauscher FG, Azmanis P, Korber N, et al. Optical coherence tomography as a diagnostic tool for retinal pathologies in avian ophthalmology. *Invest Ophthalmol Vis Sci* 2013;54:8259-69.
 37. Hayashi M, Maehara S, Ito Y, et al. Comparison between indocyanine green angiography and fluorescein angiography in normal cats. *Vet Ophthalmol* 2017;20:310-5.
 38. Menghini M, Lujan BJ, Zayit-Soudry S, et al. Correlation of outer nuclear layer thickness with cone density values in patients with retinitis pigmentosa and healthy subjects. *Invest Ophthalmol Vis Sci* 2014;56:372-81.